

Acoustic Velocity and Attenuation in Magnetorheological fluids based on an effective density fluid model

Min Shen^{1,2}, Qibai Huang¹

¹ Huazhong University of Science and Technology in Wuhan, China

² Wuhan Textile University in Wuhan, China

Abstract. Magnetorheological fluids (MRFs) represent a class of smart materials whose rheological properties change in response to the magnetic field, which resulting in the drastic change of the acoustic impedance. This paper presents an acoustic propagation model that approximates a fluid-saturated porous medium as a fluid with a bulk modulus and effective density (EDFM) to study the acoustic propagation in the MRF materials under magnetic field. The effective density fluid model derived from the Biot's theory. Some minor changes to the theory had to be applied, modeling both fluid-like and solid-like state of the MRF material. The attenuation and velocity variation of the MRF are numerical calculated. The calculated results show that for the MRF material the attenuation and velocity predicted with this effective density fluid model are close agreement with the previous predictions by Biot's theory. We demonstrate that for the MRF material acoustic prediction the effective density fluid model is an accurate alternative to full Biot's theory and is much simpler to implement.

1 Introduction

Magnetorheological fluids (MRFs) are materials whose properties change when an external electro-magnetic field is applied. They are considered as “smart materials” because their physical characteristics can be adapted to different conditions. Hence, MRFs material can be used in design of active sound barriers to control noise transmission loss and for modification of noise absorption characteristics of sound absorbing materials [1].

The MRFs consist of micron size magnetically permeable particles suspended in a carrying liquid such as the mineral or silicon oil. From the point of view of the inner structure, the particles are scattered randomly in the liquid carrier in the absence of magnetic fields shown in Figure.1(a). When a magnetic field is applied to the fluid, the particles magnetized and chain-like structures that align in the direction of the applied field as depicted in Figure.1(b). In the presence of shear strain, the particles aligned as columnar microstructure, in turn dramatically change its acoustic impedance control magnetic field. However, if the magnetic field is removed, the suspension turns to a Newtonian fluid and the transition between these two phases is highly reversible, which provides a unique feature of electric- or magnetic-field controllability of acoustic impedance of MRF. This feature has inspired the design of new active sound barriers to control noise transmission loss or as acoustic metamaterials with negative effective dynamic bulk modulus [2-3].

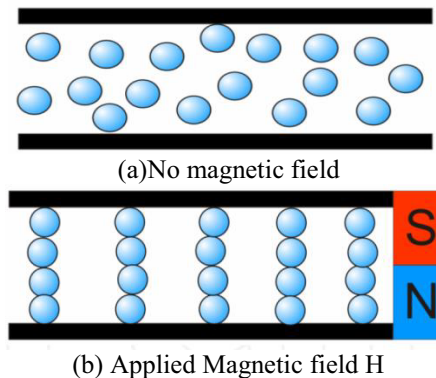


Figure.1 The MR effect:(a) the particles in the absence of magnetic fields;(b) particles magnetized and form columns when applied field;

Since the discovery of the magnetorheology, only a few works have been published in acoustic properties of the MRF. Malinovsky et al.[2-3] designed actively electro-magnetically controlled acoustic metamaterial. They construct negative mass employs mass-spring oscillator build into another mass. A lattice of such “mass-in-mass” elements could be highly attenuated for acoustic/vibration waves. An one dimensional chain model discussed based on discrete elements with effective mass density and elastic modulus. In their study, the theoretical model of acoustic wave propagation in MRF is based on one dimensional wave equation in the elastic medium.

Howarth et al[4] conducted a series of acoustic experiments at the National High Magnetic Field Laboratory in Tallahassee, Florida. The acoustic sound speed of MR fluids was measured as functions of applied magnetic field strength, normal and orthogonal field orientations, and acoustic frequency. Their presentation discussed measurement methodology and preliminary results about the MRF material.

In previous work, Shen and Huang [5] present the acoustic model of MRF materials based on the Biot-Stoll model[6-8]. The Biot's model is an useful extension of the equivalent fluids description, which takes into account the stiffness of the frame and demonstrates that two compressional waves and one shear wave can propagate in porous materials. For the case where a strong coupling exists between the fluid and the frame, the two compressional wave exhibit very different properties, and are identified as the slow wave and the fast wave. The Biot-Stoll model is a comprehensive model. It is necessary to derive an approximate equation for simplify practical application acoustic wave propagation in MRF suspensions.

This paper presents an effective density fluid model that studies the acoustic propagation in the MRF material under magnetic field to simple the Biot's model. The effective density fluid model (EDFM) approximates a fluid-saturated porous medium as a fluid with a bulk modulus and effective density derived from Biot's theory.

2 Acoustic Model

2.1 The Biot's model

When an acoustic wave propagates in a porous, elastic, solid medium saturated by a visous fluid. The Biot's model considers that two compressionl waves and one shear wave can propagate in a porous medium simultaneously[6-8]. Let u is displacement of the frame, U is displacement of the pore fluid relative to the frame.

$$u = \nabla \phi_s + \nabla \times \psi_s \quad (1)$$

$$\beta(u - U) = \nabla \phi_f + \nabla \times \psi_f \quad (2)$$

where β is the porosity. Biot's equations for the scalar potentials are then given as (using a plane wave solution $\exp[i(k \cdot x - \omega t)]$)

$$(-k^2 H) \Phi_s + k^2 C \Phi_f = (-\omega^2) \rho \Phi_s + \rho \omega^2 \Phi_f \quad (3)$$

$$(-k^2 C) \Phi_s + k^2 M \Phi_f = (-\omega^2) \rho_f \Phi_s + \omega^2 \alpha \rho_f \Phi_f / \beta + i \omega F \eta \Phi_f / \kappa \quad (4)$$

in Eqs.(3) and (4), $k = \omega / c$ is the acoustic wave number, f is the frequency, c is the speed of sound, α is the structure constant or tortusotity, η is the pore fluid viscosity, κ is the permeability.

$$\rho = \beta \rho_f + (1 - \beta) \rho_s \quad (5)$$

where ρ is the total mass density, ρ_f is the pore fluid mass density and ρ_s is the particle mass density.

The material coefficients are

$$H = [(K_r - K_b)^2 / (D - K_b)] + K_b + (4\mu / 3) \quad (6)$$

$$C = (K_r - K_b) K_r / (D - K_b), \quad (7)$$

$$M = K_r^2 / (D - K_b), \quad (8)$$

$$D = K_r [1 + \beta(K_r / K_r - 1)] \quad (9)$$

We note that K_r is the bulk modulus of individual particles and K_f is th bulk moulus of the base fluid. The parameter F represents the deviation from Poiseuille flow as frequency increases. Biot derived an expression for F that in the present notation is

$$F(\xi) = \frac{\xi T(\xi) / 4}{1 - 2i T(\xi) / \xi} \quad (10)$$

with

$$T(\xi) = \frac{(-\sqrt{i}) J_1(\xi \sqrt{i})}{J_0(\xi \sqrt{i})} \quad (11)$$

where J_1 and J_0 are cylindrical Bessel functions and

$$\xi = a \sqrt{\frac{\omega \rho_f}{\eta}} \quad (12)$$

The parameter a is the pore size parameter. Johnson et al[9]. Examined the problem of a pressure gradient applied across a porous sample and found that for a porous media consisting of nonintersecting canted tubes the relationship for a

$$a = \sqrt{\frac{8\alpha\kappa}{\beta}} \quad (13)$$

Using Eqs.(3) and (3), a fourth-order polynomial for the complex wave number k can be found. The soltion gives two different wave numbers corresponding to the Biot fast and slow waves. Both these waves show significant dispersion.

2.2 The effitive density fluid model

Taking the $K_b = \mu = 0$ limit of Biot theory is motivated by the fact that for magnetorheological fluids the frame and shear moduli are much lower than the other moduli[10-12].

Using Eqs.(6-8), it is easy to shown that, when K_b and μ are set to zero.

$$H = C = M = \left(\frac{1 - \beta}{K_r} + \frac{\beta}{K_f} \right)^{-1} \quad (14)$$

The result states that the compressibility is a linear function of the concentration of the particles in a suspension as assumed by Urick in

$$(-k^2 H) \phi_s + k^2 H \phi_f = (-\omega^2) \rho \phi_s + \rho_f \omega^2 \phi_f \quad (15)$$

$$(-k^2 H) \phi_s + k^2 H \phi_f = (-\omega^2) \rho_f \phi_s + \frac{\omega^2 \alpha \rho_f}{\beta} \phi_f + \frac{i \omega^2 F \eta}{\kappa} \phi_f \quad (16)$$

Using Eqs.(15) and (16), a second-order equation for the wave number k can be found. This solution and the relation from Eq.(3-4) that $k=\omega / c$ can be used to find that

$$k^2 = \frac{\omega^2 \rho_{\text{eff}}(\omega)}{H} \quad (17)$$

where

$$\rho_{\text{eff}}(\omega) = \rho_f \left(\frac{\alpha(1-\beta)\rho_s + \beta(\alpha-1)\rho_f + \frac{i\beta\rho F\eta}{\rho_f \omega \kappa}}{\beta(1-\beta)\rho_s + (\alpha-2\beta+\beta^2)\rho_f + \frac{i\beta F\eta}{\omega \kappa}} \right) \quad (18)$$

is a complex effective density.

3 Numerical Results and Discussion

To verify the correctness of this model, the longitudinal wave velocity and attenuation coefficient of the MRF are calculated. Using the equations in the preceding section, the longitudinal wave velocity and attenuation coefficient are calculated for MRF-132DG material. Table 1 lists the parameters of the model for the MRF investigated which is typical of MRF-132DG manufactured by Lord Corporation. All parameters of MRF in braces are either directly supplied by the manufacturer or have been calculated[5]. The calculations for the linear equations are numerically performed. For the MRF description, the fluid bulk modulus can be assumed purely elastic, because in our case the base fluid is low-viscosity silicone oil.

Figure 2 shows the real and imaginary parts of the effective density as a function of frequency from 10Hz to 100KHz. The physical reason for the transition between these two values can be understood from Biot theory[6-7]. At low frequencies the pore size parameter is much smaller than the viscous skin depth and there is no relative motion between the grains and the water. At high frequencies the skin depth is much smaller than the pore size parameter (typical pore radius) and it is the tortuosity determines the relative motion of the fluid and solid.

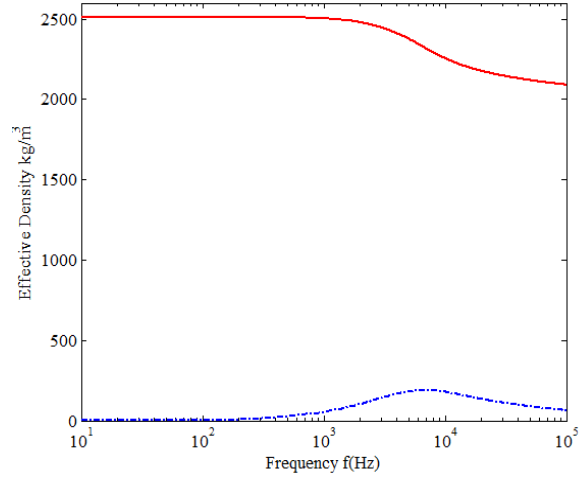


Figure.2 The real (solid curve) and imaginary (dot-dashed) parts of the effective density given in Eq.(12) for the MRFs in Table 1.

Table.1 The EDFM model Parameters of MRF-132DG

Parameters	Symbol(Unit)	MRF
Solid density	$\rho_r(\text{kg} / \text{m}^3)$	3160
Fluid density	$\rho_f(\text{kg} / \text{m}^3)$	1000
Grain bulk modulus	$K'_r(N / \text{m}^2)$	1.26×10^{11}
Volumetric Specific loss	δ_{kr}	0.4
Fluid bulk modulus	$K'_f(N / \text{m}^2)$	9.8×10^8
Grain diameter	$d_m(\text{m})$	$1 \square 10 \times 10^{-6}$
Fluid viscosity	$\eta(Ns / \text{m}^2)$	$0.075 \square 10^6$
Frame shear modulus	$G'_b(N / \text{m}^2)$	$0 \square 8 \times 10^6$
Shear specific loss	δ_{Gb}	$0 \square 0.5$
Frame bulk modulus	$K'_b(N / \text{m}^2)$	$0 \square 4 \times 10^8$
Volumetric specific loss	δ_{kb}	$0 \square 0.5$
Porosity	β	$0.1 \square 0.5$
Permeability	$B_0(\text{m}^2)$	4×10^{-12}

Figure 3 and 4 shows the sound speed and attenuation as a function of frequency for both Biot model (solid lines) were used to derive the dispersion equation and the EDFM (dot dashed line-Eq.(18)). Both models produce similar dispersion in sound speed. However, the EDFM predict speeds that are about 10m/s slower at the lowest frequencies and about 5m/s slower at the highest frequencies. The average sound speed error is approximately 0.5% over the frequency range plotted. The bulk and shear moduli of the frame obviously increase in sound speed slightly. It is demonstrated that the sound speeds predicted with this

effective density fluid model are very close to the predictions of Biot theory and much simpler than the full Biot model.

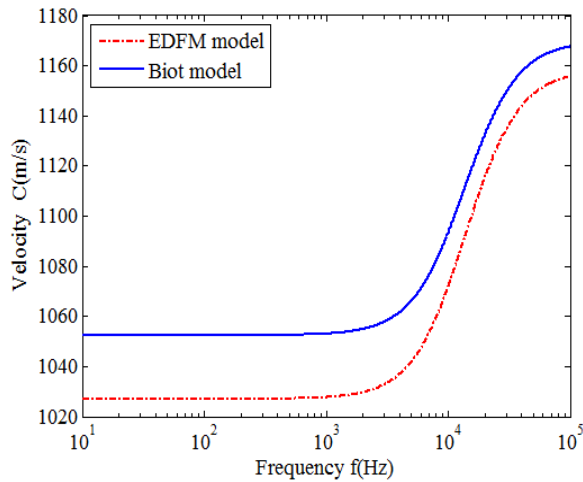


Figure.3 The sound speed as a function of frequency calculated using the Biot model (solid curve) and the effective density fluid model(dashed curve) for the MRFs in Table 1.

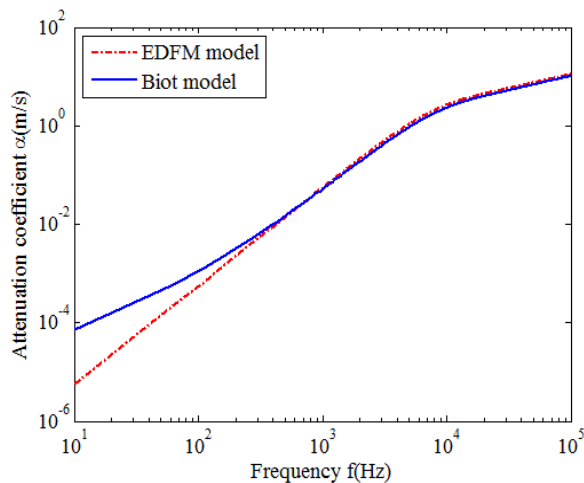


Figure.4 Attenuation as a function of frequency calculated using the Biot model(solid) curve and the effective density fluid model (dashed curve) for the MRFs in Table.1

Figure 4 shows that the attenuation predicted by the EDFM is slightly lower at the lowest frequencies plotted. This discrepancy increases as the frequency is reduced below the range plotted due to internal frictional effects of the frame. The attenuation due to frame moduli varies linearly with frequency. Thus, at low enough frequencies the frame attenuation will begin to become important.

The continuous line was obtained by averaging just the density values, taking into account that for a dilute suspension one can neglect the effects of suspended particles on the elastic properties of the composite medium.

Figure 5 shows the three-dimensional representations of longitudinal wave velocity in the frequency of 1Hz to 1MHz, and the viscosity range of 0.087 to 10² when placed in a weak magnetic field. The viscosity of MRF

trends to saturation above 10³. It is seen from Fig.5 that the longitudinal wave velocity increases dependent on the field strength, but when the viscosity above the 60, the wave velocity is nearly kept 1750m/s and independent on frequency.

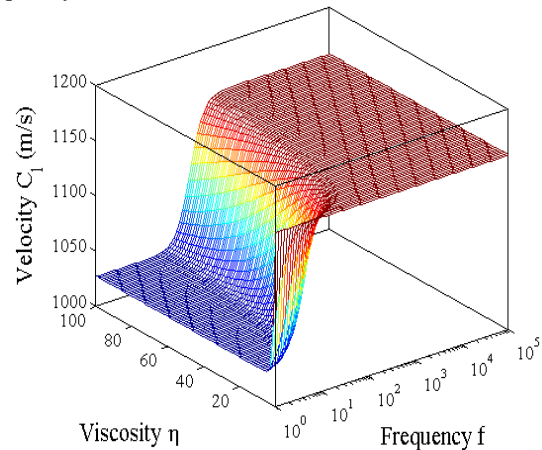


Figure.5 Three-dimensional representation of the longitudinal wave velocity as functions of viscosity and frequency for MRF

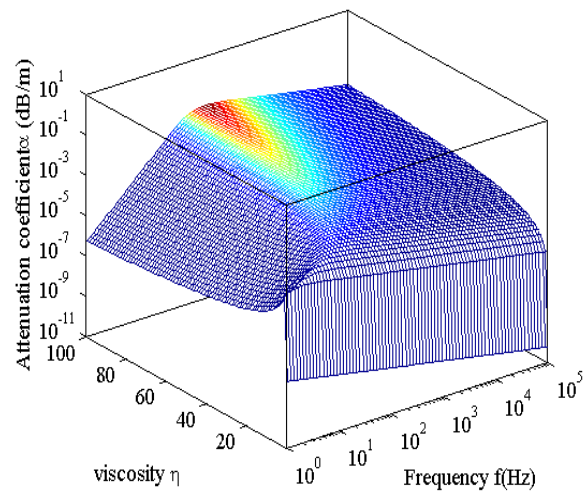


Figure.6 Three-dimensional representation of the attenuation as functions of viscosity and frequency for MRF

Figure 6 shows the three-dimensional representations of attenuation coefficient variation changes with frequency and viscosity. It is seen from Fig.6 that the attenuation coefficient increases as the viscosity increases above the frequency 10²Hz. However, there is a sharp jump on the curve below the frequency 10²Hz, the attenuation coefficient is very complex dependent on both frequency and field strength. Hence, the MRF has better active acoustic absorption properties with the applied magnetic field in the mid-high frequency range. We should improve the dynamic acoustic absorption performance in the low frequency range by appropriately select other geometric parameters of the MRF.

Figure 7 shows the three-dimensional representations of sound speed variation changes with frequency and porosity. It is seen from Fig.7 that the sound speed increases as the porosity decreases from the frequency

10Hz to 100k Hz. The velocity increases occurring over a broad band of frequency. It is well known that in a colloidal suspension, only one longitudinal mode can exist when an elastic excitation propagates in it if the wavelength is much larger than the characteristic size of the suspended particles.

In calculating the sound speed, we assume that in the first mode, the elastic perturbation propagates through channels of almost clear fluid. Provided that the perturbation wavelength is much larger than the characteristic size of the iron particles.

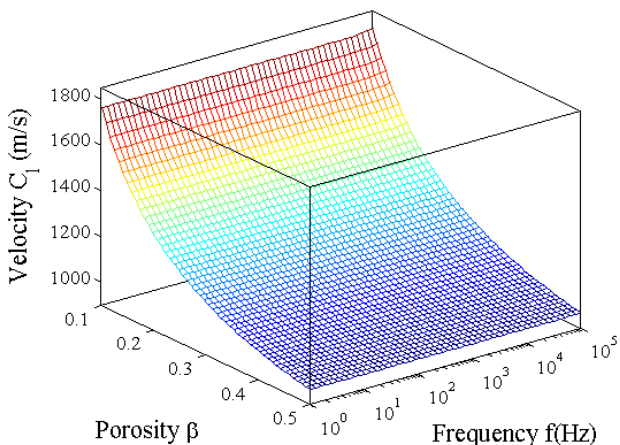


Figure.7 Three-dimensional representation of the sound speed as functions of porosity and frequency for MRF

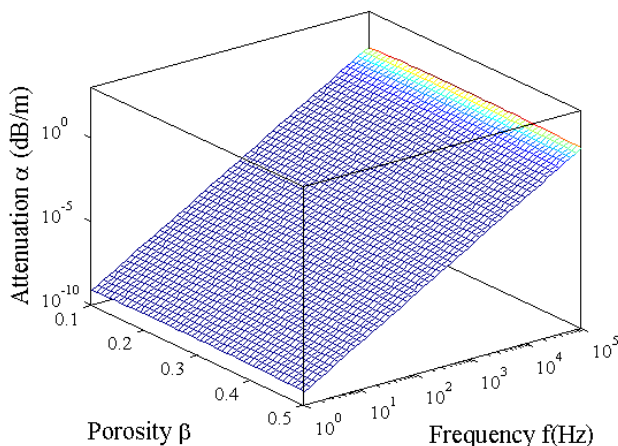


Figure.8 Three-dimensional representation of the attenuation coefficient as functions of porosity and frequency for MRF

Figure8 shows the three-dimensional representations of attenuation coefficient variation changes with frequency and porosity. It is seen from Fig.8 that the attenuation coefficient is almost increasing as the porosity increases. We can assume that the effect of iron spheres in this dilute dispersion is only of inertial nature,i.e, the elastic properties of the fluid will not be affected by the presence of a few non-interacting particles. Then, neglecting dissipation effects, the only average which must be considered in this calculation.

The present research was supported by the China National Science Foundation (No.51175195 , No.51505344). The magneto-rheological investigations were performed at State Key Laboratory of Digital Manufacturing Equipment and Technology, Huazhong University of Science and Technology,Wuhan,China.

References

1. M.Szary, The analytical model of rheological fluid for vibration and noise control, Proceedings of Meetings on Acoustics, Montreal, Canada, 19(2013):1-8.
2. S.Malinnovsky and D.M.Donskoy, Electro-magnetically controlled acoustic metamaterials with adaptive properties, Journal of the Acoustical Society of America, 132(2012):2866-2872.
3. D.M.Donskoy, V.S.Malinnovsky, Broadband acoustic metamaterials with electro-magnetically controlled properties, Proceedings of Meetings on Acoustics, Montreal,Canada, 19(2013):1-8.
4. T.R.Howarth,F.Fratantonio,J.E.Boisvert,A.Bruno,C.L.Scandrett,W.M.Wynn and P.S.Davis, Acoustic behavior of magnetorheological fluids in magnetic fields, Journal of the acoustical society of America, 13(2011):2359.
5. M.Shen and Q.B.Huang, Acoustic properties of magnetorheological fluids under magnetic fields, Applied Mechanical and Materials,721(2015):818-823.
6. M.A.Biot, Theory of propagation of elastic waves in a fluid-saturated porous solid, Part I:Low frequency range, Journal of the Acoustical Society of America, 28,(1956):168-178.
7. M.A.Biot, Theory of propagation of elastic waves in a fluid-saturated porous solid, Part II:Higher frequency range, Journal of the Acoustical Society of America,28(1956):179-191.
8. R.D.Stoll, Acoustic waves in ocean sediments, Geophysics, 42,4,(1977):715.
9. D.L.Johnson, J.Koplik and R.Dashen, Theory of dynamic permeability and tortuosity in fluid-saturated porous media, Journal of Fluid Mechanics, 176(1087):379-402.
10. K.L.Williams, An effective density fluid model for acoustic propagation in sediments derived from Biot theory, Journal of the Acoustical Society of America, 110,5(2001),2276-2280.
11. K.L.Williams and D.R.Jackson, Bistatic bottom scattering:Model, experiments, and model/data comparison, Journal of the Acoustical Society of America, 103,1,(1998):169-181.
12. K.L Willams, D.R Jackson, E.I Thorsos,Tang and J, S.G Schock, Comparison of sound speed and attenuation measured in a sandy sediment predictions based on the Biot theory of porous media,IEEE Journal Ocean Engineering, 27,3(2002): 413-428.

ACKNOWLEDGEMENTS